Results

Harmonic analysis of the scalar satellite magnetic residuals confirms a strong M2 ocean signal (Fig. 7).

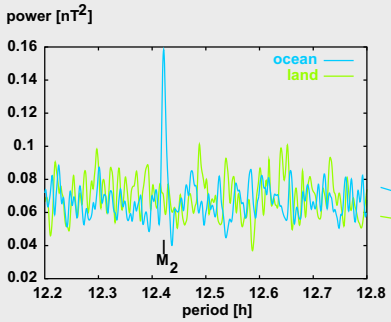

Fig. 7: The power spectrum of magnetic residuals has a clear M2 ocean peak.

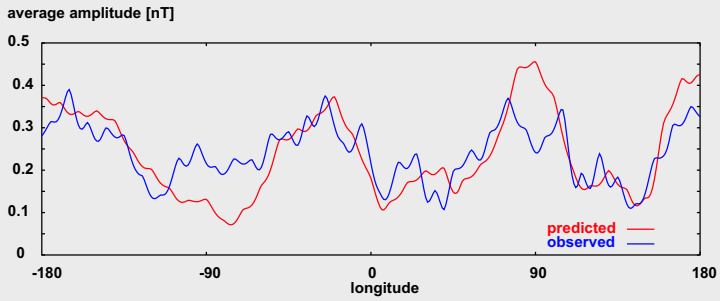

Fig. 8: Meridionally averaged amplitudes.

Figure 8 compares the meridionally averaged amplitudes of the observed and predicted magnetic signal.

The M2 harmonic signal can be described by a complex function of location. The real part of this function (corresponding to a location of the moon at 0 or 180 degrees longitude) is displayed in Figure 9 against the corresponding prediction from the ocean flow model. The full time-varying comparison is displayed in the accompanying movie.

The observed M2 signal is in remarkable agreement with our numerical prediction, proving that the observed signal is indeed due to ocean flow, rather than induction in a static conductor. Observed and predicted signals were derived independently. In particular, the model has not been adapted to the observed signal in any way.

East/West stripes and a non-vanishing signal over the source-free land areas is largely an effect of the along-track filtering (applied to both model and observed data) which removes North/South trending signal and transports signal from the ocean onto the land areas. Another effect of filtering is to reduce the overall signal amplitude.

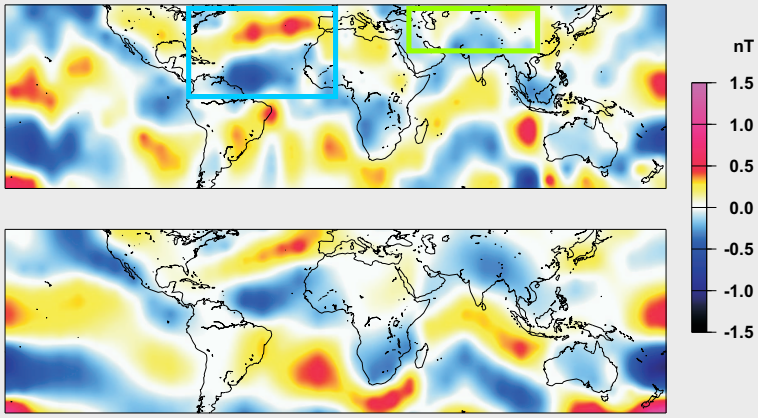

Fig. 9: Observed (top) versus predicted (bottom) real part of the M2 harmonic constituency in the magnetic field intensity residuals.

Numerical prediction

Using a thin-sheet formulation (1) we integrate the motional induction equation governing the magnetic vector component perpendicular to the sheet. Mantle and crust are assumed to be insulating. Sediment conductances are derived from the Laske and Masters (7) sediment thickness map following a method previously described (8). Ocean conductivity is assumed to have a constant value of 3.2 S/m.

The model is depth averaged and replaced with an infinitely thin spherical shell. Using the main field model CO2 (5), the magnetic forcing term from ocean flow is first calculated on a ½-degree resolution grid and then interpolated on to the coarser 2 degree grid of our model. To obtain numerical solutions, the equations are discretized using a conservative finite-difference approximation on a spherical grid with 2x2-degree resolution with 26 unequally spaced shells. The linear system of equations is solved using an iterative ILU method, yielding the scalar potential of the magnetic field at satellite altitude.

along-track filtering

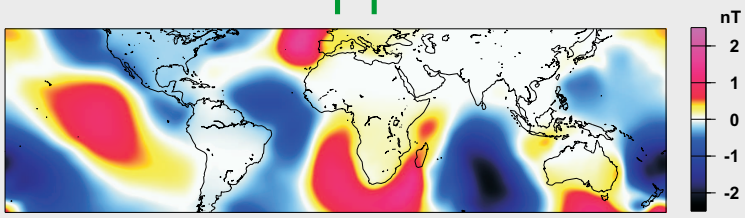

Fig. 10: Real part of the magnetic field intensity anomaly predicted from M2 tidal ocean flow. Before comparing this prediction with the observed signal it has to be filtered in the same way as the measured data.

integration of motional induction equation

Tidal ocean flow model

Tidal flow is taken from the M2 constituency of the TPXO.5.1 ocean model (9), derived TOPEX/Poseidon satellite radar altimetry data.

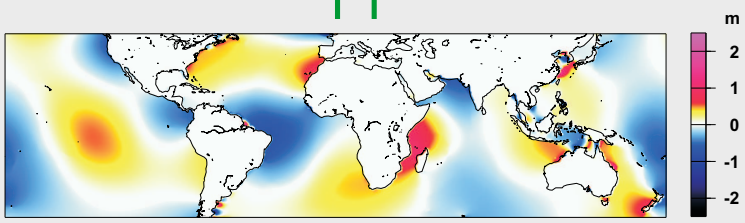

Fig. 11: Real part of sea surface height due to M2 tidal ocean flow as given by model TPXO.5.2 (c)

Conclusions

The identification of this ocean dynamo signal has important implications: In broader terms, it encourages future studies to assess the feasibility of monitoring ocean flow from space using magnetic field satellites. A more immediate consequence, however, is that oceanic signals must be incorporated into geomagnetic field models. Indeed, with recent advances in internal/external field separation the ocean flow signal is now the strongest remaining signal in the low latitude magnetic residuals which has not yet been modelled. Correcting magnetic readings for predictable ocean flow signals could significantly raise the detectability of small scale crustal magnetization.

References

1. T. B. Sanford, Journal of Geophysical Research 76, 3476 (1971).
2. A. D. Chave, D. S. Luther, Journal of Geophysical Research 95, 7185 (1990).
3. R. H. Tyler, L. A. Mysak, Geophysical and Astrophysical Fluid Dynamics 80, 167 (1995).
4. S. R. C. Malin, Journal of the Royal Astronomical Society, 21, 447-455 (1970).
5. R. Holme, N. Olsen, M. Rother, H. Lühr, CO2 -A CHAMP magnetic field model, in "CHAMP Mission Results I", (Springer, Berlin, 2002). in print.
6. S. Maus, M. Rother, R. Holme, H. Lühr, N. Olsen, V. Haak, Geoph. Res. Lett. 29, 10.1029/2001GL013685 (2002).
7. G. Laske, G. Masters, EOS Trans. AGU 78, F483 (1997).
8. M. E. Everett, S. Constable, C. Constable. Modelling 3D induction effects in satellite data, in Proc. of the 2nd Int. Symp. on 3D Electromagnetics (1999), pp. 63–67.
9. G. D. Egbert, A. F. Bennet, M. G. G. Foreman, Journal of Geophysical Research 99, 24821 (1994).

Links

Supplementary material: www.gfz-potsdam.de/pb2/pb23/SatMag/ocean_tides.html
CHAMP mission: http://op.gfz-potsdam.de/champ/
GFZ space borne magnetometry: www.gfz-potsdam.de/pb2/pb23/SatMag/me.html
G. Egbert's tidal model: www.oce.orst.edu/po/ocean.html
NOAA tides online: http://tidesonline.nos.noaa.gov/monitor.html
Ocean electrodynamics: http://sirena.apl.washington.edu/